African Journal of Mathematics and Statistics Studies
ISSN: 2689-5323
Volume 7, Issue 3, 2024 (pp. 95-108)
www.abjournals.org

ANALYSIS OF A REACTIVE FLOW IN ROTATING CONCENTRIC CYLINDERS

O. M. Badejo and O. K. Ogunbamike*

Department of Mathematical Sciences, School of Science, Olusegun Agagu University of Science and Technology, Okitipupa, Nigeria.

*Corresponding Author's Email: ok.ogunbamike@oaustech.edu.ng

Cite this article:

Badejo O. M., Ogunbamike O. K. (2024), Analysis of a Reactive flow in Rotating Concentric Cylinders. African Journal of Mathematics and Statistics Studies 7(3), 95-108. DOI: 10.52589/AJMSS-P7ZCWKPD

Manuscript History

Received: 26 Jun 2023

Accepted: 3 Sep 2023

Published: 8 Aug 2024

ABSTRACT: *The introduction of bearing was to bring conveniences because it reduces the friction and whirring at the joint, especially for complex moving machines. Bearing was produced for smooth usage but the contrary is derived once they are being used on uneven roads or subjected to overloading. This may not sustain lives again but put them at risk which may lead to death sometimes. The governing equations were modeled based on the reviewed work, linearized and adopted with Hartmann number (Ha), Pressure gradient (G) and other parameters like Darcy number (Da), Prandtl number (Pr), Eckert number (Ec), Suction parameter ($\boldsymbol{V_0}$) and Reynolds number (Re) but they were made to be equal to one (1) throughout the research work. The energy equation with reactive terms was tested and the value of G was at an interval of 0.50 from 0.00 to 2.00 while the Ha were considered at an interval of 1.00 from 1.00 to 10.00. Perturbation method was used to linearize the equations and was solved numerically using the semi-implicit finite difference scheme with Maple 18 software. When the value of Ha was observed from* $\boldsymbol{0.00 mms^{-1}}$ *to* $\boldsymbol{20.00 mms^{-1}}$ *with* $\boldsymbol{0 \leq G \leq 2}$*, it shows an increase in velocity which depicts reduction in the free flow of fluids in the rotating concentric cylinder. When* $\boldsymbol{G > 0}$*, there is smooth fluid flow in the system and the results show that the higher the value of G the more the fluid flow (*$\boldsymbol{0 \leq G \leq 2}$*). The temperature of G on Ha reduces as the value of Ha on G increases suggesting that* $\boldsymbol{G \geq 10}$ *can be used to stabilize the system's temperature. The result of Ha on other parameters for both velocity and temperature increase as the value of Ha increases. Also, the maximum temperature of the system with reactive flow is very high; ranging from* $\boldsymbol{0.05 - 0.30\ deg}$C*. The results were in agreement with related works in literature.*

KEYWORDS: Annulus, Concentric cylinder, Pressure gradient; Magnetic field, Reactive flow.

Article DOI: 10.52589/AJMSS-P7ZCWKPD
DOI URL: https://doi.org/10.52589/AJMSS-P7ZCWKPD

African Journal of Mathematics and Statistics Studies
ISSN: 2689-5323
Volume 7, Issue 3, 2024 (pp. 95-108)

www.abjournals.org

INTRODUCTION

Both animate and inanimate body systems experienced reactive flow in daily life. The rate at which humans feel changes in body temperature subject to ongoing body activity at a particular time is very important when considering reactive flow in living organisms. Administering medication to the body system such as injection and intake of water or food into the human system are some of the things to look at when working on reactive flow. Ball and socket joint in animals is fully mobile because it contains a small amount of synovial fluid under the control of muscles, ligaments and tendons. Just like bearing in machines. Bearings are machine elements that allow components to move smoothly with respect to each other. Bearings are used to support large skyscrapers to move during earthquakes and they enable the finest of watches to tick away. There exist two types of bearings, mainly contact and non-contact. Contact-type bearings have mechanical contact between elements, and they include sliding, rolling, and flexural bearings. However, mechanical contact is when stiffness normal to the direction of motion is very high, but wear or fatigue can limit its life spans. The non-contact bearings include externally pressurized and hydrodynamic fluid-film (liquid, air, mixed phase) and magnetic bearings. Several related works in literature revealed that researchers mostly concentrated on either the cylinders stationary while the other rotating. In this work, both cylinders are to be rotating in opposite directions and the effect of Ha, G and reactive parameters will also be considered. Although viscous drag occurs when fluids are present; however, life can be virtually infinite if the external power units required to operate them do not fail [1]. Each type of bearing has its own application area, and thus design engineers are familiar with different types of bearings, their applications and limitations. As with all other types of machine elements, it is important to understand the fundamental operating principles of different bearings in order to select the right bearing for the intended application. Note that the fundamental principles of design are of particular importance to the proper use of bearings in machines. Ali [2] studied concentric annular flows of Newtonian fluids in vertical and horizontal arrangements based on CFD simulations, but failed to quantify the effects of internal shaft rotation. Also, a mathematical model was presented for the steady, axisymmetric, magnetohydrodynamic (MHD) flow of a viscous, Newtonian, incompressible, electrically-conducting liquid in a highly porous regime intercalated between two concentric rotating cylinders in the presence of a radial magnetic field. The porous medium is modeled using a Darcy-Forchheimer drag force approach in simulating the impedance effects of the porous medium fibers at both low and higher velocities [3]. Sankar et al. [4] studied numerically a natural convection of a low number electrically conducting fluid under the influence of either axial or radial magnetic field in a vertical cylindrical annulus. Renkatachalappa et al. [5] worked seriously on numerical computations to investigate the effect of axial or radial magnetic field on the double-diffusive natural convection in a vertical cylindrical annular cavity. Not up to a decade, Aberkane et al. [6] estimated the effect of an axial magnetic field imposed on incompressible flow of electrically conductive fluid between two horizontal coaxial cylinders. The imposed magnetic field is assumed to be uniform and constant. The effect of heat generation due to viscous dissipation is also taken into consideration. Darbhashayanam et al. [7] analyzed the Joule heating effect on the viscous fluid flow over a porous sheet stretching exponentially by employing convective boundary condition and it was observed from the investigation that the rate of heat transfer reduces with Joule heating and enhances with increasing Biot number.

Article DOI: 10.52589/AJMSS-P7ZCWKPD
DOI URL: https://doi.org/10.52589/AJMSS-P7ZCWKPD

Dulal et al. [8] studied the interaction of convection and thermal radiation on an unsteady hydromagnetic heat and mass transfer for a viscous fluid past a semi-infinite vertical moving plate embedded in a porous media in the presence of heat absorption and first order chemical reaction of the species. The results are presented graphically and in tabular forms to study the effects of various physical parameters. The analysis of the hydro-magnetic Nanofluid boundary layer flow over a rotating disk in a porous medium with a constant velocity in the presence of hall current and thermal radiation, velocity profiles and temperature profiles of the boundary layer are plotted and investigated in detail [9]. Edrogan [10] also analyzed the unsteady fluid flow by non-coaxial rotations of a disk and a fluid at infinity. The effect of viscous dissipation and Joule heating on unsteady MHD flow over a stretching sheet saturated in porous medium was investigated by Sharma et al. [11]. The effect of these parameters on fluid velocity, fluid temperature, skin-friction coefficient and Nusselt number are presented through figures and discussed numerically. Okedayo et al. [12] studied the effects of viscous dissipation on unsteady flow of a reactive fluid with a temperature dependent viscosity and thermal conductivity through a horizontal channel filled with porous material. The coupled nonlinear differential equations governing the flow were solved numerically using the semi-implicit finite difference scheme and the result clearly stated the effects of viscous dissipation.

Darbhasayanam et al. [13] studied the laminar mixed convective flow of an incompressible chemically reacting nanofluid in an annulus between two concentric cylinders by considering the Joule heating effect. The maximum values of Bejan number *Be* are observed at the center of the annulus due to more contribution of heat transfer irreversibility on entropy generation and the minimum value is near the cylinders due to more contribution of fluid friction irreversibility on entropy generation with an increase in parameters.

Recently, Badejo et al. [14] studied the magnetic field effects on reactive flow in rotating concentric cylinder where several values of Hartmann number (Ha) were tested on both velocity and the temperature of the system and it was observed that higher value of Ha reduces the fluid flow and also increases the temperature of the system. Usman et al. [15] worked on the effects of pressure gradient on reactive flow in a rotating concentric cylinder and it was observed that the higher the value of pressure gradient (G) in the system, there is a reality of free flow of fluid with low level of temperature. Hence in this study, the analysis of a reactive flow in rotating concentric cylinders has been conducted. Pullepudi et al. [16] investigated some of the fluid flow interaction, interferences in flow and vortex dynamics which are typically found in compact heat exchangers, cooling of electronic equipment, nuclear reactor fuel rods, cooling towers, chimney stacks, offshore structures, hot-wire anemometry and flow control. Its structures are subjected to air or water flows and therefore experience flow induced forces which can lead to their failure over a long period of time. Basically, with respect to the free stream direction, the configuration of two cylinders can be classified as tandem, side-by-side and staggered arrangements. The Reynolds Averaged Navier Stokes (RANS) equations are used to compute the flow and Eulerian model is used to understand phase change situations. The validation of the results compares favorably with those in literature. In the present study, nucleate boiling has been the cause of heat and mass transfer between the phases. Orientation of cylinders in a specific arrangement has significant impact on phase change and volume fraction of both liquid and vapor phase. The effect of orientation of a cylinder in an arrangement and its rotation on the volume fraction of each phase has been the focus. Hence two different arrangements such as tandem and staggered are considered during the computation to understand the phase change of liquid to vapor phase over a cylinder whose surface is heated

Article DOI: 10.52589/AJMSS-P7ZCWKPD
DOI URL: https://doi.org/10.52589/AJMSS-P7ZCWKPD

African Journal of Mathematics and Statistics Studies
ISSN: 2689-5323
Volume 7, Issue 3, 2024 (pp. 95-108)

to a certain temperature (above the saturation temperature of vapor). Most recently, Qin et al. [17] studied a novel tracked chassis for the road rail vehicle with a multi-cylinder hydropneumatic suspension system, which can better adapt to rough terrains and enhance the vehicle ride performance. If it is based on this hydropneumatic suspension design, the single-cylinder mathematical model is derived and validated by experimental data. An in-plane multi-body dynamics (MBD) model and road model were established, combined with the hydropneumatic suspension model with the inclusion of the Lugre friction force. Virtual tests are conducted to investigate the effects of different initial gas volumes, varied diameters and damping pipe lengths on the ride performance. The results indicate that improper damping pipe diameter and charge gas volume will deteriorate the ride performance, which provides a useful reference for the optimization design and control of the hydropneumatic system. Computer simulations of vehicle dynamics become more complex when a vehicle movement takes place on the uneven road surface, such that a case of two problems were solved. The first one was about road surface modeling and the second treated determines a place of interaction of reaction forces of the road on the vehicle wheels. It was also observed that triangular irregular networks (TIN) surface was used for modeling surface unevenness and the author's algorithm based on the efficient kd-tree data structure was developed for determining a place of an application like road surface reaction forces. The solution presented was in agreement with the literature [18]. The effect of an axial magnetic field imposed on incompressible flow of electrically conductive fluid between two horizontal coaxial cylinders was studied. The imposed magnetic field assumed uniformity and constant. The effect of heat generation due to viscous dissipation was also taken into account. The inner and outer cylinders were maintained at different uniform temperatures and concentrations. It was also observed that movement of fluid is due to rotation of the cylinder with constant speed. An exact solution of the governing equations for momentum and energy were obtained in the form of Bessel functions. A finite difference implicit scheme was used in the numerical solution to solve the governing equations of convection flow and mass transfer. The velocity, concentration and temperature distributions were obtained with and without the magnetic field. The results show that for different values of the Ha, the velocity and concentration between the two cylinders decreases as the Ha increases [19].

Mathematical Formulation

Fig. 2.1 shows the upper view and movement of concentric annulus cylinder in opposite directions, where $r_1, r_2, r_1\omega$ and $r_2\omega$ are the inner radius, outer radius, velocity of the inner and velocity of outer annulus cylinder respectively.

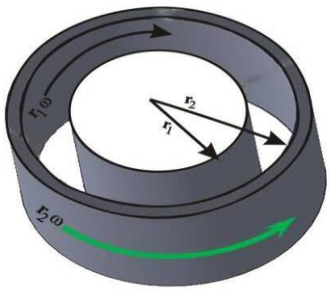

Fig. 2.1: Schematic representation of two rotating concentric cylinders

Article DOI: 10.52589/AJMSS-P7ZCWKPD
DOI URL: https://doi.org/10.52589/AJMSS-P7ZCWKPD

African Journal of Mathematics and Statistics Studies
ISSN: 2689-5323
Volume 7, Issue 3, 2024 (pp. 95-108)
www.abjournals.org

This section considered a system with and without reactive term flow in between concentric cylinders rotating simultaneously, unsteady state, laminar, and fully developed flow of fluids for which the density and the viscosity are constant. The governing partial differential equations in cylindrical coordinate for this case are:

Continuity equation

$$\frac{\partial}{\partial r}(ur) = 0 \tag{1}$$

u - Momentum equation

$$\frac{\partial u}{\partial t} = V\left[\frac{\partial^2 u}{\partial r^2} + \frac{\partial}{\partial r}\left(\frac{u}{r}\right)\right] - \frac{1}{\rho}\frac{\partial P}{\partial r} - \frac{\sigma u {B_0}^2}{\rho} - \frac{Vu}{K} - \frac{\Gamma u^2}{K} \tag{2}$$

v - Momentum equation

$$\frac{\partial v}{\partial t} = V\left[\frac{\partial^2 v}{\partial r^2} + \frac{\partial}{\partial r}\left(\frac{v}{r}\right)\right] - \frac{1}{\rho}\frac{\partial P}{\partial r} - \frac{\sigma v {B_0}^2}{\rho} - \frac{Vv}{K} - \frac{\Gamma v^2}{K} \tag{3}$$

w - Momentum equation

$$\frac{\partial w}{\partial t} = V\left[\frac{\partial^2 w}{\partial r^2} + \frac{\partial}{\partial r}\left(\frac{w}{r}\right)\right] - \frac{1}{\rho}\frac{\partial P}{\partial r} - \frac{\sigma w {B_0}^2}{\rho} - \frac{Vw}{K} - \frac{\Gamma w^2}{K} \tag{4}$$

Given that:

For the inner cylinder

$$v = w = 0, u = r_1\omega \tag{5}$$

For the outer cylinder

$$v = w = 0, u = r_2\omega \tag{6}$$

Substituting equations (5) and (6) into equations (2), (3) and (4) only equation (2) will be visible.

Therefore, u is the velocity, V is the fluid kinematic viscosity, r is the radius, $\frac{u}{r}$ is the rotating parameter in the governing partial differential equations. Similar procedure was done on the energy equation for a reactive flow of rotating concentric cylinder with different coordinates to yield:

$$\frac{\partial T}{\partial t} = \frac{u}{r}\frac{\partial}{\partial r}\left(r\frac{\partial T}{\partial r}\right)K + \mu\left(\frac{\partial u}{\partial r} - \frac{u}{r}\right)^2 \tag{7}$$

Therefore, the governing Navier-Stoke equations are (1), (2), (7) and

Article DOI: 10.52589/AJMSS-P7ZCWKPD
DOI URL: https://doi.org/10.52589/AJMSS-P7ZCWKPD

African Journal of Mathematics and Statistics Studies
ISSN: 2689-5323
Volume 7, Issue 3, 2024 (pp. 95-108)
www.abjournals.org

$$\frac{\partial T}{\partial t} = \frac{u}{r}\frac{\partial}{\partial r}\left(r\frac{\partial T}{\partial r}\right)K + \mu\left(\frac{\partial u}{\partial r} - \frac{u}{r}\right)^2 + QC_0Ae^{\left(\frac{E}{RT}\right)} \quad (8)$$

Equations (7) and (8) are the energy equations without and with reactive terms respectively. The last term in (8) is the reactive term. The Boundary Conditions are:

$$r = r_1, \quad u = r_1\omega\,, \; r = r_2, \quad u = r_2\omega \quad (9)$$

Dimensionless Parameters

$$U = \frac{u}{\omega b}, R = \frac{r}{b}, T = \frac{t}{t_0}, \theta = \frac{T}{T_0}, V_0 = \frac{\omega}{b}, V = \frac{\mu}{\rho} \quad (10)$$

These can also be written in these forms

$$u = U\omega b \quad r = Rb \quad t = Tt_0 \quad T = \theta T_0 \quad \omega = \quad V_0 b \quad \mu = V\rho \quad (11)$$

Substituting equation (11) into equations (2) to yields the dimensionalized momentum equation

$$\frac{\partial U}{\partial T} = \frac{\partial^2 U}{\partial R^2} + \frac{1}{Re}\frac{\partial}{\partial R}\left(\frac{U}{R}\right) + \frac{G}{Re} - \frac{Ha^2}{Re}U - \frac{1}{Da}U - \frac{Fs\,Re}{Da}U^2 \quad (12)$$

Substituting equation (11) into equations (7) yields the dimensionalized energy equation without reactive term

$$\frac{\partial \theta}{\partial T} = \frac{V_0}{Pr}\left(\frac{U}{R}\right)\frac{\partial}{\partial R}\left(R\frac{\partial \theta}{\partial R}\right) + Ec\left[\left(\frac{\partial U}{\partial R}\right)^2 - 2\frac{U}{R}\left(\frac{\partial \quad U}{\partial R}\right) + \left(\frac{U}{R}\right)^2\right] \quad (13)$$

Substituting equation (11) into equations (8) yields the dimensionalized energy equation with reactive term

$$\frac{\partial \theta}{\partial T} = \frac{V_0}{Pr}\left(\frac{U}{R}\right)\frac{\partial}{\partial R}\left(R\frac{\partial \theta}{\partial R}\right) + Ec\left[\left(\frac{\partial U}{\partial R}\right)^2 - 2\frac{U}{R}\left(\frac{\partial U}{\partial R}\right) + \left(\frac{U}{R}\right)^2\right] + \gamma e^{\left(\frac{1}{\varepsilon}\right)} \quad (14)$$

Therefore:

Γ: Forchheimer Geometric Inertial drag parameter

$$Fs = \frac{\Gamma}{b}$$

V_0: Suction Parameter

$$V_0 = \frac{\omega_2}{b}$$

G: Pressure Gradient

$$G = -\frac{\partial P}{\partial R}$$

γ: Frank-Kamenetskii Parameter

Article DOI: 10.52589/AJMSS-P7ZCWKPD
DOI URL: https://doi.org/10.52589/AJMSS-P7ZCWKPD

$$\gamma = \frac{QC_0t_0}{T_0b^2}$$

Re: Reynolds Number

$$Re = \frac{\omega_2 b^2}{\nu}\nu$$

Ha: Hartmann Number

$$Ha^2 = \frac{\sigma B_0^2 b^2}{\mu}$$

Da: Darcy Number

$$Da = \frac{r}{b^2}$$

Pr: Prandtl Number

$$Pr = \frac{b^2}{Kt_0}$$

Ec: Eckert Number

$$Ec = \frac{\mu\omega_2^2 t_0}{T_0 b^2}$$

ε: Activation Energy

$$\varepsilon = \frac{RT_0}{E}$$

B_0: Magnetic Field

σ: Fluid Electrical Conductivity

ν: Fluid Kinematic Viscosity

ρ: Fluid Density

k: Porus Medium Permeability

Q: Heat Reaction

A: Rate Constant

R: Universal Gas Constant

C_0: Initial Concentrating of the Reacting Species

The Boundary Conditions also yield

Article DOI: 10.52589/AJMSS-P7ZCWKPD
DOI URL: https://doi.org/10.52589/AJMSS-P7ZCWKPD

African Journal of Mathematics and Statistics Studies
ISSN: 2689-5323
Volume 7, Issue 3, 2024 (pp. 95-108)
www.abjournals.org

$$R = \frac{r_1}{b} \qquad U = \frac{r_1\omega}{\omega_2 b} \qquad R = \frac{r_2}{b} \qquad U = \frac{r_2\omega}{\omega_2 b} \tag{15}$$

Factorizing equation (12) becomes:

$$\frac{\partial U}{\partial T} = \frac{\partial^2 U}{\partial R^2} - \frac{1}{Re}\frac{U}{R} - \left[\frac{Ha^2}{Re} + \frac{1}{Da}\right]U - \frac{FsRe}{Da}U^2 + \frac{G}{Re} \tag{16}$$

If $M = \left[\frac{a^2}{Re} + \frac{1}{Da}\right]$; $N = \frac{FsRe}{Da}$; $Q = \frac{G}{Re}$

Therefore, the unsteady equation (16) reduces to:

$$\frac{\partial U}{\partial T} = \frac{\partial^2 U}{\partial R^2} + \frac{1}{Re}\frac{1}{R}\frac{\partial U}{\partial R} - \frac{1}{Re}\frac{1}{R}U - MU - NU^2 + Q \tag{17}$$

The initial boundary conditions (IBC) are:

$$U(0.5,t) = 0.3, U(1,t) = 0.6, U(R,0) = 0, \theta(0.5,t) = 0, \theta(1,t) = 0, \theta(R,0) = 0 \tag{18}$$

UNSTEADY STATE OF REACTIVE FLOW SYSTEM

Equation (17) needs to be perturbed because of its non-linearity in nature. Hence, the velocity U is assumed to be:

$$U = U_0 + \alpha U_1 \tag{19}$$

Hence,

$$\frac{dU}{dR} = \frac{dU_0}{dR} + \alpha\frac{dU_1}{dR} \tag{20}$$

$$\frac{\partial^2 U}{\partial R^2} = \frac{d^2 U_0}{dR^2} + \alpha\frac{d^2 U_1}{dR^2} \tag{21}$$

Substituting equations (19), (20) and (21) into equation (17) with further simplification yields

$$\frac{\partial^2 U_0}{\partial R^2} + \frac{1}{Re}\frac{1}{R}\frac{\partial U_0}{\partial R} - \frac{1}{Re}\frac{1}{R}U_0 - MU_0 + Q = 0 \tag{22}$$

$$\frac{\partial U_1}{\partial T} = \frac{\partial^2 U_1}{\partial R^2} + \frac{1}{Re}\frac{1}{R}\frac{\partial U_1}{\partial R} - \frac{1}{Re}\frac{1}{R}U_1 - MU_1 - {U_0}^2 \tag{23}$$

Let, $P = \frac{V_0}{Pr}$

Therefore, equation (13) becomes

Article DOI: 10.52589/AJMSS-P7ZCWKPD
DOI URL: https://doi.org/10.52589/AJMSS-P7ZCWKPD

African Journal of Mathematics and Statistics Studies
ISSN: 2689-5323
Volume 7, Issue 3, 2024 (pp. 95-108)
www.abjournals.org

$$\frac{\partial\theta}{\partial t} = PU\frac{\partial^2\theta}{\partial R^2} + P\left(\frac{U}{R}\right)\frac{\partial\theta}{\partial R} + Ec\left(\frac{\partial U}{\partial R}\right)^2 - 2Ec\frac{U}{R}\left(\frac{\partial U}{\partial R}\right) + Ec\left(\frac{U}{R}\right)^2 \quad (24)$$

Further simplification of equation (24) yields:

$$\frac{1}{U}\frac{\partial\theta}{\partial t} = P\frac{\partial^2\theta}{\partial R^2} + \frac{P}{R}\frac{\partial\theta}{\partial R} + Ec\frac{1}{U}\left(\frac{\partial U}{\partial R}\right)^2 - 2Ec\frac{1}{R}\left(\frac{\partial U}{\partial R}\right) + Ec\frac{U}{R^2} \quad (25)$$

The temperature θ, is assumed to be

$$\theta = \theta_0 + \alpha\theta_1 \quad (26)$$

Hence,

$$\frac{d\theta}{dR} = \frac{d\theta_0}{dR} + \alpha\frac{d\theta_1}{dR} \quad (27)$$

$$\frac{\partial^2\theta}{\partial R^2} = \frac{d^2\theta_0}{dR^2} + \alpha\frac{d^2\theta_1}{dR^2} \quad (28)$$

Substituting equations (26), (27) and (28) into (25) with further simplification yields:

$$\frac{\partial\theta}{\partial t} = P\frac{\partial^2\theta_0}{\partial R^2} + \left(\frac{P}{R}\right) \quad (29)$$

$$P\frac{\partial^2\theta_1}{\partial R^2} + \left(\frac{P}{R}\right)\frac{\partial\theta_1}{\partial R} + \frac{U_0}{R^2} = 0 \quad (30)$$

Similarly, equation (14) results to:

$$\frac{\partial\theta}{\partial t} = P\frac{\partial^2\theta_0}{\partial R^2} + \left(\frac{P}{R}\right)\frac{\partial\theta_0}{\partial R} \quad (31)$$

$$P\frac{\partial^2\theta_1}{\partial R^2} + \left(\frac{P}{R}\right)\frac{\partial\theta_1}{\partial R} + \frac{U_0}{R^2} + \gamma e^{\left(\frac{1}{\varepsilon}\right)} = 0 \quad (32)$$

RESULTS AND DISCUSSION

This study has shown that reactive flow in a rotating concentric cylinder (annulus) is very important in our day-to-day activities, especially when we consider its benefits in all aspects of human life and the environment at large. Considering the results below, Ha which reveals the effect of magnetic force in this study shows that as the Ha increases on the other parameters the temperature of the system also increases (Fig. 4b, Fig. 5b and Fig. 6b). This also increases the rate of fluid flow within the proximity of the system (Fig. 4a, Fig. 5a and Fig. 6a) which could lead to shortage of fluid in the concentric cylinder due to overheating. This signifies the effects of uneven roads and overloading of moving vehicles on rotating concentric cylinders.

It was also observed that as the G increases, the temperature of the system decreases for all parameters (Fig. 1b, Fig. 2b and Fig. 3b) while its velocity increases (Fig. 1a, Fig. 2a and Fig. 3a), indicating free flow of fluid in the rotating concentric cylinder with low temperature making the fluid stay longer in the system. It was observed that the system without the reactive

Article DOI: 10.52589/AJMSS-P7ZCWKPD
DOI URL: https://doi.org/10.52589/AJMSS-P7ZCWKPD

African Journal of Mathematics and Statistics Studies
ISSN: 2689-5323
Volume 7, Issue 3, 2024 (pp. 95-108)
www.abjournals.org

term operates with less temperature but is unstable sometimes because of the viscosity of the fluid in the rotating concentric cylinders. This may cause the system not to work perfectly, especially when the climate is cold with high viscosity. It revealed that the fluid in the rotating concentric cylinder lacks smooth flow and efficiency. The Ha increases the temperature and also the Da, Pr and Ec. The G can be used to reduce the high temperature of a system using a rotating concentric cylinder. If it is possible, the space that could allow enough free flow of fluid within the rotating concentric cylinder and right viscosity specification of fluid should be encouraged for the users.

Considering the components of the reactive term, it shows that all flowing fluid has the composition of the reactive term and will only be sensed or observed when there is excess workload which usually increases the magnetic forces. The temperature and velocity profile of G and Ha for parameters like, Da for porous median, Pr for heat convection and Ec for dissipation of energy are also similar. Therefore, systems without reactive terms may not experience excess workload when moving on even a road.

It was also observed that the system with reactive term does not work under perfect condition, that is why uneven road and excess load generate more heat than the system without reactive term.

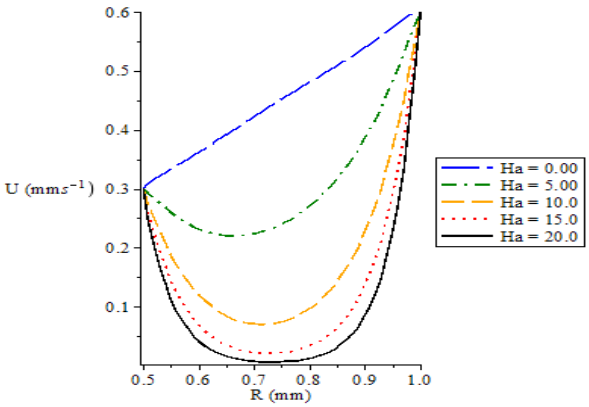

Fig.1a: Velocity profile for values of Hartmann number (Ha) when $\Re = 1$, $Da = 1$, $G = 0$, $Fs = 0.5$ & $V_0 = 1$.

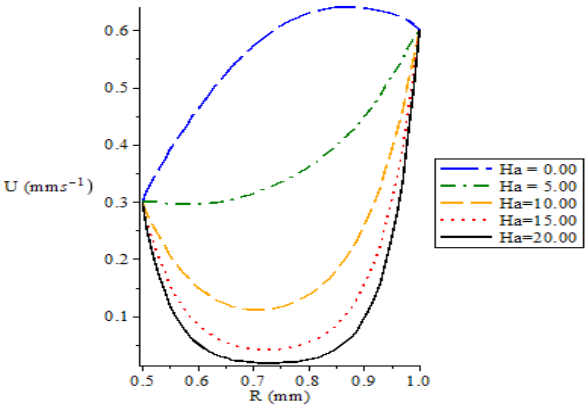

Fig.2a: Velocity profile for values of Hartmann number (Ha) with reactive term, when $\Re = 1$, $Da = 1$, $G = 5$, $Fs = 0.5$ & $V_0 = 1$.

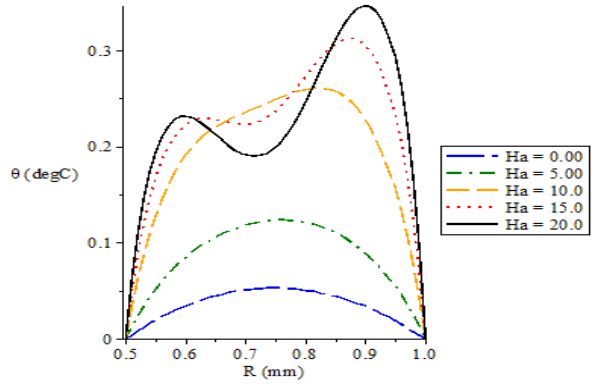

Fig.1b: The Temperature profile θ (deg C) versus Cylindrical Radius R (mm) for values of Hartmann number (Ha) with reactive term, when $Ec = 1$, $\Re = 1$, $Da = 1$, $G = 0$, $Fs = 0.5$, $V_0 = 1$ & $Pr = 1$

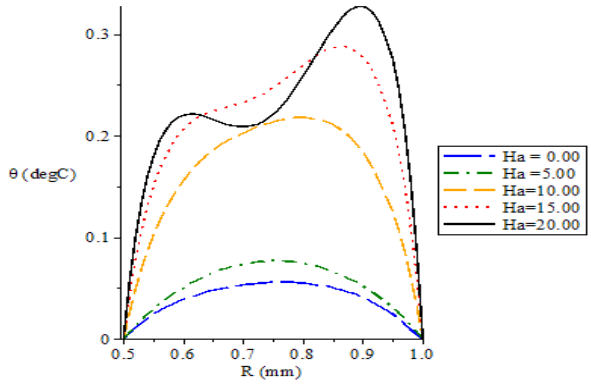

Fig. 2b: The Temperature profile θ (deg C) versus Cylindrical Radius R (mm) for values of Hartmann number (Ha) with reactive term, when $Ec = 1$, $\Re = 1$, $Da = 1$, $G = 5$, $Fs = 0.5$, $V_0 = 1$ & $Pr = 1$

Article DOI: 10.52589/AJMSS-P7ZCWKPD
DOI URL: https://doi.org/10.52589/AJMSS-P7ZCWKPD

African Journal of Mathematics and Statistics Studies
ISSN: 2689-5323
Volume 7, Issue 3, 2024 (pp. 95-108)
www.abjournals.org

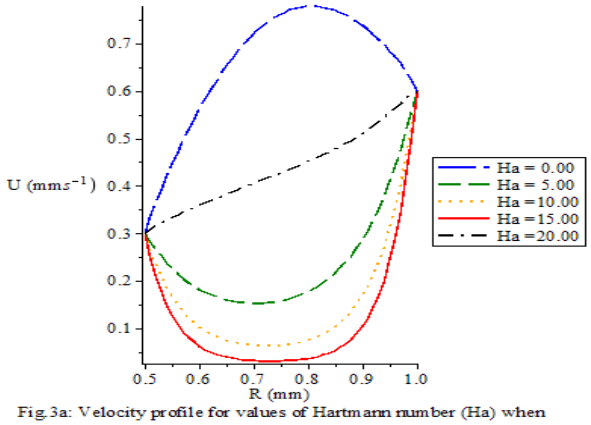

Fig.3a: Velocity profile for values of Hartmann number (Ha) when $\Re = 1$, $Da = 1$, $G = 10$, $Fs = 0.5$ & $V_0 = 1$.

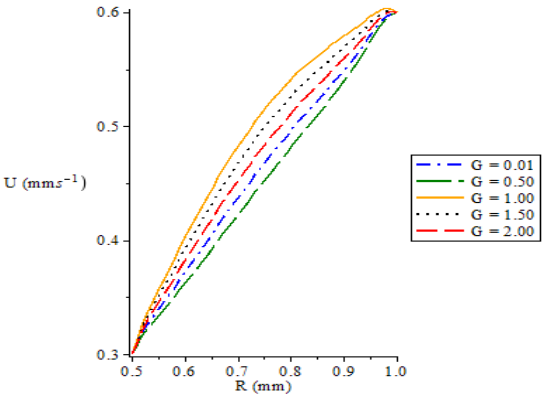

Fig.4a: Velocity profile for values of Pressure Gradient (G) when $\Re = 1$, $Da = 1$, $Ha = 0$, $Fs = 0.5$ & $V_0 = 1$.

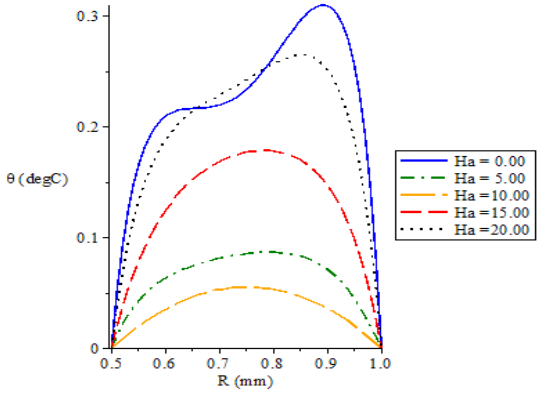

Fig.3b: Temperature profile for values of Hartmann number (Ha) with reactive term, when $Ec = 1$, $\Re = 1$, $Da = 1$, $G = 10$, $Fs = 0.5$, $V_0 = 1$ & $Pr = 1$

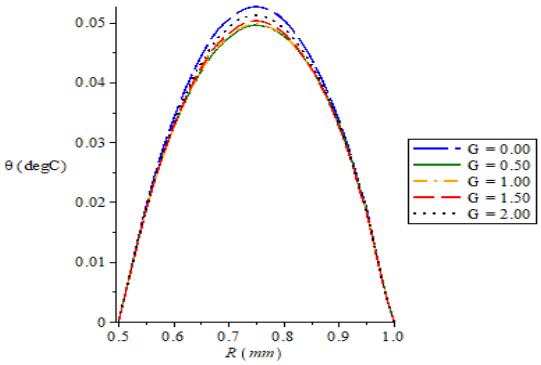

Fig. 4b: The Temperature profile θ (deg C) versus Cylindrical Radius R (mm) for values of Pressure Gradient (G) with reactive term, when $Ec = 1$, $\Re = 1$, $Da = 1$, $Ha = 0$, $Fs = 0.5$, $V_0 = 1$ & $Pr = 1$

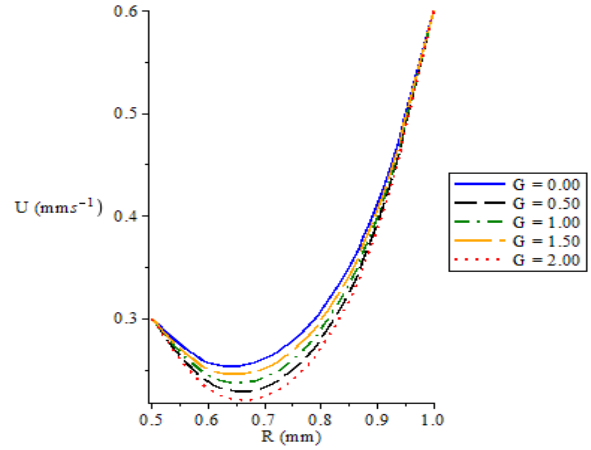

Fig.5a: Velocity profile for values of Pressure Gradient (G) when $\Re = 1$, $Da = 1$, $Ha = 5$, $Fs = 0.5$ & $V_0 = 1$.

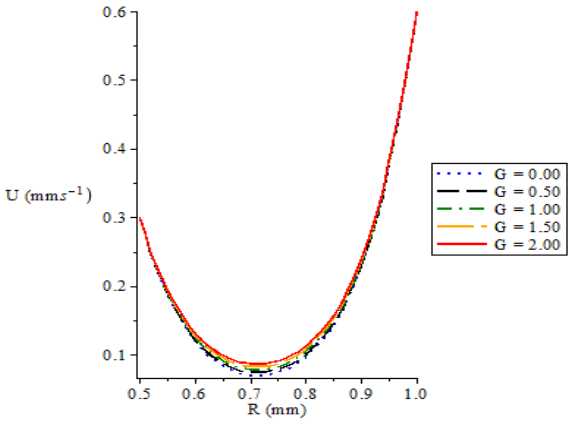

Fig.6a: Velocity profile for values of Pressure Gradient (G) when $\Re = 1$, $Da = 1$, $Ha = 10$, $Fs = 0.5$ & $V_0 = 1$.

Article DOI: 10.52589/AJMSS-P7ZCWKPD
DOI URL: https://doi.org/10.52589/AJMSS-P7ZCWKPD

African Journal of Mathematics and Statistics Studies
ISSN: 2689-5323
Volume 7, Issue 3, 2024 (pp. 95-108)
www.abjournals.org

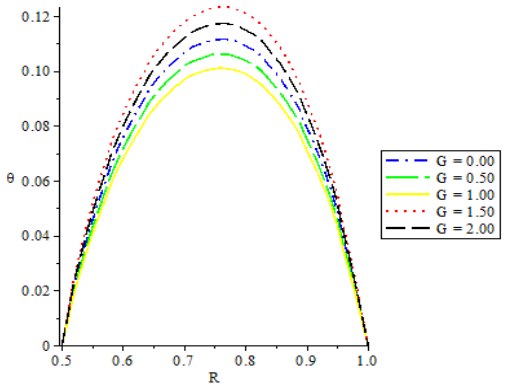

Fig. 5b The Temperature profile for values of Pressure Gradient (G) with reactive term, when
$Ec = 1$, $\Re = 1$, $Da = 1$, $Ha = 5$, $Fs = 0.5$, $V_0 = 1$ & $Pr = 1$

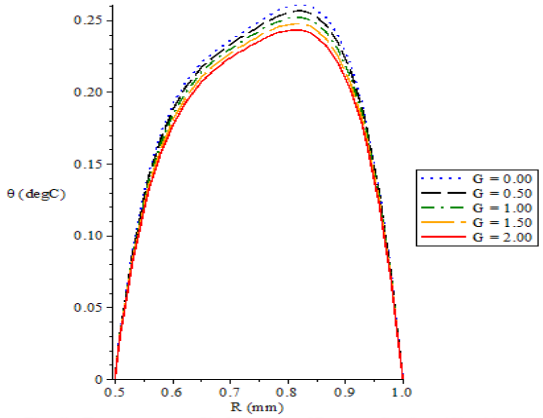

Fig. 6b: Temperature profile for values of Pressure Gradient (G) with reactive term, when $Ec = 1$, $\Re = 1$, $Da = 1$, $Ha = 10$, $Fs = 0.5$, $V_0 = 1$ & $Pr = 1$

CONCLUSION

The magnetic field, a subset of Ha, increases the temperature which signifies the usage of rotating concentric cylinders on uneven roads and overloading of moving vehicles and machines. G reduces the temperature implying usage and applications of wheel's hub, rotor, brake drum and bearings on smooth roads. Unsteady flow showed that time can determine the result of each parameter and it can be used to adjust and set time for limit temperature and the rate of fluid flow in the rotating concentric cylinder. Therefore, if there is humming or whirring noise while vehicles or machines are working, it is an indicator for a time-check or a replacement. Furthermore, there is a need to pay more attention to the specification of the fluid (viscosity) especially during the climate, and the environment where the system is being used must always be considered before the usage or replacement. It should also be noted that bearings are classified broadly according to the type of operations, therefore the motion allowed the directions of the loads (forces) applied to its parts. Finally, it is observed that time is very important because usage of bearings differ from one user to the other. Therefore, it is always advisable to look for long and smooth alternative roads rather than accessing uneven roads. Da, Pr and Ec are important to the above dimensionalized equations and without the parameters, the equations like this cannot be achieved or model properly, though this work does not consider other parameters except G and Ha.

Article DOI: 10.52589/AJMSS-P7ZCWKPD
DOI URL: https://doi.org/10.52589/AJMSS-P7ZCWKPD

REFERENCES

[1] A. Jeanneau, J. Herder, T. Laliberte and C. Gosselin, A Compliant Rolling Contact Joint and its Application in a 3-DOF Planar Paralle Mechanism with Kinematic Analysis, *Proc. DETC'04*, ASME 2004 DETC, Salt Lake City, Utah, USA.

[2] A. W. Ali, The Effect of inner Cylinder Rotating on the Fluid Dynamics of Non-Newtonian, *Brazilian Journal of Chemical Engineering*, 31(4), 2002, http://dx.doi.org/10.1590/0104-6632.20140314s00002871.

[3] O.A. Beg, O.D. Makinde, J.Z. Swapan,. and S.K. Ghosh, Hydroagnetic viscous flow in a rotating annular high-porosity medium with nonlinear forcheimer drag effects: numerical study, *World Journal of Modelling and Simulation*, 8(2), 2012, 83-95.

[4] M. Sankar, M. Venkatachalappa and S. Shivakumara, Effect of magnetic field on natural convection in a vertical
cylindrical annulus, *International Journal of Engineering Science*, 44, 2006, 1556-1.

[5] M. D. Venkatachalappa and S. M. Younghae, Effect of magnetic field on the heat and mass transfer in a vertical annulus, *International Journal of Engineering Science*, 49, 2011, 262-278.

[6] S. Aberkane, I. Malika, M. Moderres and G. Abderrahmane, Effect of axial magnetic field on the heat and mass transfer in rotating annulus, *International Journal of Physical Sciences*, 9(16), 2014, 368-379.

[7] S. Darbhashayanam and J. Pashikanti, Effect of Joule heating on the flow over an exponentially stretching sheet with convective thermal condition, *Springer Mathematical Sciences*, 2019, https://doi.org/10.1007/s40096-019-0290-8.

[8] P. Dulal and T. Babulal, Combined effects of Joule heating and chemical reaction on unsteady magnetohydrodynamic mixed convection of a viscous dissipating fluid over a vertical plate in porous media with thermal radiation, *Elsevier*, 54, 20113016-3036.

[9] M.S. Abdel-wahed and T.G. Emam, Effect of Joule Heating and Hall Current on MHD Flow of a Nanofluid due to a Rotating Disk with Viscous Dissipation, *Thermal Science*, 2016, DOI: 10.2298/tsci160312218a.

[10] M.E. Erdogan, Unsteady flow of a viscous fluid due to non-coaxial rotations of a disk and a fluid at infinity, *International Journal of Non-Linear Mechanics: 32*, 1997, 285–290.

[11] P.R. Sharma and S. Sinha, Combined Effects of Viscous Dissipation and Joule Heating on Unsteady MHD Flow and Heat Transfer over a Stretching Sheet Saturated in Porous Medium, *Annals of Pure and Applied Mathematics*, 14(3), 2017, 387-399.

[12] T. G. Okedayo, S. O. Abah and R.T. Abah, Viscous dissipation effects on the reactive flow of a temperature dependent viscosity and thermal conductivity through a porous channel. *ABACUS*, 41(2), 2014, 74-81.

[13] S. Darbhasayanam and M.D. Shafeeurrahman, Joule Heating Effect on Entropy Generation in MHD Mixed Convection Flow of Chemically Reacting Nanofluid between Two Concentric Cylinders, *International Journal of Heat and Technology*: 35(3), 2017, 487-497.

[14] O. M. Badejo and M.A. Usman, Magnetic field effects on reactive flow in rotating concentric cylinder, *The Coast, Journal of Faculty of Science, OAUSTECH*, 2(1), 2019, 288-295.

[15] M. A. Usman and O. M. Badejo, Effects of pressure gradient on reactive flow in rotating concentric cylinders, *The Coast, Journal of Faculty of Science, OAUSTECH*, 1(2), 2019, 225-231.

Article DOI: 10.52589/AJMSS-P7ZCWKPD
DOI URL: https://doi.org/10.52589/AJMSS-P7ZCWKPD

[16] R. Pullepudi and S.K. Maharana, Numerical Investigation on Effect of Orientation and Rotation on Liquid Vapor Phase Change around a Cylinder in Staggered Arrangement, *International Journal of Applied Engineering Research* 14(1); 2019, 220-227
[17] B. Qin, R. Zeng, X. Li and J. Yang, Design and Performance Analysis of the Hydro pneumatic Suspension System for a Novel Road-Rail Vehicle. *Applied Science,* 2021, https://doi.org/10.3390/ app11052221
[18] T. Szymon a The effect of the reactive parameter will also be considered.nd W. Kornel, An Effective Algorithm of Uneven Road Surface Modelling and Calculating Reaction Forces for a Vehicle Dynamics Simulation, *Coating* 2021, 11, 535 https://doi.org/10.3390/coatings11050535.
[19] S. Aberkane M. Ihdene M. Moderes A. and Ghezal, Effect of axial magnetic field on the heat and mass transfer in rotating annulus. International Journal of Physical Science, 2014, 9(16), 368-379

Article DOI: 10.52589/AJMSS-P7ZCWKPD
DOI URL: https://doi.org/10.52589/AJMSS-P7ZCWKPD